

REINFORCEMENT OF MASONRY ARCHES BY FRP MATERIALS: EXPERIMENTAL TESTS AND NUMERICAL INVESTIGATIONS

Raimondo Luciano, University of Cassino, Cassino, ITALY

Sonia Marfia, University of Cassino, Cassino, ITALY

Elio Sacco, University of Cassino, Cassino, ITALY

Introduction

Advanced fiber reinforced plastic (FRP) composite materials appear good candidates to substitute standard materials in the strengthening and in the reinforcement of masonry structures. In fact, these materials present a combination of excellent properties, such as low weight, immunity to corrosion, possibility of formation in very long lengths, high mechanical strength and stiffness. They can be successfully applied to the tensile zones of structural members by using epoxy adhesives. Moreover, FRP materials are very simple to install (resulting in low labor costs) and they are also removable.

The possibility of adopting FRP composites for the strengthening of masonry was initially investigated by Croci et al. [1]. They presented the results of experimental tests conducted on wall specimens reinforced by vertical or inclined FRP materials. Experimental investigations were developed by Schwegler [2] in order to evaluate the mechanical response of masonry walls reinforced by carbon fiber sheets or conventional woven fabric bonded on the surfaces. In particular, Schwegler demonstrated the effectiveness of this technique through full-scale, both in-plane and out-of-plane, cyclic testing of one-story masonry walls. Further experimental investigations devoted to the study of the behavior of masonry specimens strengthened with epoxy-bonded glass fabrics were developed by Saadatmanesh [3] and by Ehsani [4]. Cyclic tests on half-scale masonry walls, reinforced by epoxy-bonded overlays made of unidirectional carbon fibers, were performed by Laursen et al. [5]. A full-scale reinforced masonry building, subjected to simulated seismic loading, was tested by Seible [6], who demonstrated the effectiveness of the reinforcement in increasing the strength, reducing the shear deformations and improving the overall structural ductility. Triantafillou [7] and Triantafillou and Fardis [8] studied the effectiveness of FRP tendons used to apply circumferential prestresses for strengthening historical masonry structures. Luciano and Sacco [9, 10] and Marfia and Sacco [11] proposed micromechanical models for studying the behavior of masonry elements reinforced by FRP sheets.

In the last few years, great interest was devoted to the reinforcement of arches and vaults by FRP materials. In fact, aramid fiber reinforced composites were adopted to restore the vaults of the “Basilica di San Francesco di Assisi” [12], since urgent measures were required immediately after the earthquake to prevent the total collapse of the tympanum and of the vaults. Investigations on the static of arches reinforced on the intrados or on the extrados were developed by Como et al. [13].

In the present paper, an application of FRP materials for the reinforcement of masonry arches is presented. The study is justified by the possibility of reinforcing an existing old masonry structure,

sited in the historical town center of Atina (Italy). The effectiveness of the carbon FRP reinforcement is investigated by performing experimental tests on full-scale unreinforced and reinforced arches. Moreover, numerical investigations are performed using the finite element code FEAP, developed by Taylor [14]. Material models, available in FEAP, are adopted and new damage models are implemented to simulate the masonry and reinforcement material behavior.

Results obtained from the stress analyses are discussed and put in comparison with the experimental behavior of the full scale arch.

Case Study

The masonry structure considered in the present study represents the full scale sample of one of the arch belonging to the arcade located at the last floor of “Palazzo Bologna” in Atina, which is a little roman town of central Italy. The arcade is composed by round arches that are very damaged and, hence, they need to be strengthened. The arches are constituted by homogeneous compact limestone blocks without mortar. Each arch of the arcade has a span of about 1600 mm. The blocks, that compose the structure, are characterized by different lengths, but constant rectangular cross-section $b \times h$ with height $h = 300$ mm and base $b = 160$ mm. Experimental tests performed on small samples of the compact limestone constituting the arches, allow to evaluate the compression strength of the block material σ_c equal about to 60 MPa.

In order to reinforce the damaged arches, FRP advanced composite materials are considered. Because of aesthetic reasons, the FRP sheets can be applied only on the extrados and on the internal lateral surface of the structure. To evaluate the effectiveness of the strengthening intervention and to investigate the influence of the FRP on the overall structural behavior of the arch, laboratory experimental tests and numerical analyses are performed on unreinforced and reinforced full scale arches.

In particular, one of the arch of the arcade is selected in “Palazzo Bologna” and it is reproduced in the laboratory. Because of the difficulty in recovering the homogeneous compact limestone constituting the blocks of “Palazzo Bologna”, a suitable concrete is used for the laboratory construction. Thus, a concrete characterized by a compression strength of about 60 MPa, comparable with the experimental limestone strength obtained for the masonry specimens, is mixed. The mechanical properties of the mixed concrete are:

Young modulus: $E_m=40000$ MPa Poisson coefficient: $\nu_m=0.2$
Compression strength: $\sigma_c=60$ MPa Material density: $\rho_m=0.0022$ Kg/mm³

Sheets of carbon FRP material, characterized by a thickness of $0.18 \div 0.25$ mm, are used. The properties of the FRP composite are:

Young modulus: $E_r=400000$ MPa Carbon fiber strength: $\sigma_r=3500$ MPa

Thus, concrete blocks, characterized by the same geometry, material strength and elastic

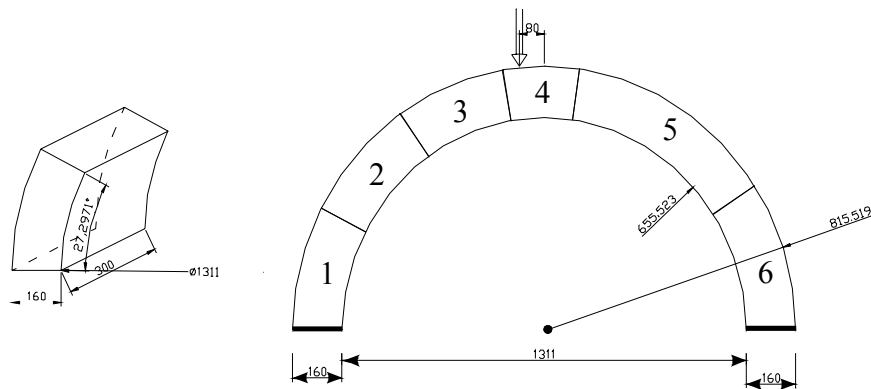


Figure 1. Geometry of the arch and of a single block.

modulus of the selected arch, are made and assembled in the laboratory prototypes. In fact, several prototypes of the selected arch are realized and tested.

The arches reproduced in the laboratory are subjected to a point-wise load, with an eccentricity of 80 mm with respect to the keystone, as shown in figure 1, where the arch geometry is reported and it is quoted in millimeters. This load condition is very easy to reproduce in the experimental phase and, furthermore, it appears to be particularly severe for the structure; then, the eccentric load appears suitable for evaluating the increase in the bearing capacity due to the FRP reinforcement.

Experimental Behavior Of The Arch

Experimental tests are developed applying the external force by means of the hydraulic jack. Initially, experiments are performed on the unreinforced arch. In figure 2, the picture illustrating the four hinges mechanism, corresponding to arch collapse, is reported. The failure occurs for a load of about 2 kN.

Then, two arches characterized by different reinforcements are tested. The first arch is reinforced by FRP sheets on the extrados and on one of the two lateral surfaces. In particular, the arch is reinforced by two overlapped sheets, characterized by a width of 200 mm, on the extrados and by a single sheet, with a width of 100 mm, on the internal lateral surface. The behavior of arch is monitored by twelve displacement transducers (LVDTs), able to measure horizontal and vertical displacements. The decohesion of the composite applied on the lateral surface occurs for low values of the applied load, without any damage of the concrete. Thus, the lateral reinforcement appears useless. The first visible crack appears at the intrados, near the keystone, for a load equal to 100 kN. The collapse load is equal to 290 kN, with a local failure of the keystone, as illustrated in Figure 3.

On the basis of the results obtained from the first experimental test, the second arch to be tested is reinforced only on the extrados. In order to increase the cohesion between the concrete blocks and the FRP composite, the concrete surface is treated to get a high roughness. Then, the

sample is reinforced with great care in mixing and applying the epoxy resin. The collapse is reached once again at the keystone, for a load of about 190 kN. In Figure 4, it can be noted that the keystone is ejected so that the arch is transformed in two cantilever beams. The ultimate behavior of the arch is different from the first test because of the presence of an initial defect in the structure, located close to the load application point. In fact, this defect causes a different cracking pattern in the arch even for low level of the applied force.

A more detailed description of the above outlined experiments is reported in reference [15], where analytical models able to predict the behavior of unreinforced and reinforced arches are



Figure 2. The four hinges mechanism for the unreinforced arch.



Figure 3. Failure of the first reinforced arch.



Figure 4. Collapse of the second reinforced arch.

proposed.

It can be noted that in both the experimental tests the collapse occurs for the limited strength in compression of the concrete; in fact, FRP composite remains undamaged during the whole loading process. Thus, the nonlinear behavior and the failure of concrete have to be taken into account in the finite element analyses, while the reinforcement can be considered as a linear elastic material.

Material Models

Several material models are considered for the numerical study of the arch. Next, a very short discussion on the adopted models is reported.

The behavior of the interfaces between adjacent blocks is modeled considering the unilateral effect and assuming that slip cannot occur. In particular, the no-tension material model [16] is adopted to simulate the unilateral behavior of the interface.

The behavior of the masonry blocks is studied adopting:

- the linear elastic constitutive model;
- the no-tension model; it considers no tensile strength with linear elastic behavior in compression;
- the elasto-plastic Von Mises model with a yield stress equal to 60 MPa,
- the damage model in compression; in particular, a linear softening stress-strain relationship, characterized by the damage stress threshold equal to 60 MPa is considered.

It can be emphasized that the linear elastic model is able to simulate the masonry behavior for very low values of the stress field. The no-tension model can be successfully adopted to study masonry structures presenting tensile cracks, but it cannot be used to investigate the behavior of constructions subjected to compressive failure. The elasto-plastic Von Mises model could describe with satisfactory approximation the behavior of the concrete in compression when plane stress state occurs. In particular, to reproduce the behavior of cementitious materials, a nonlinear stress-strain material response is assumed for very low values of the compression as proposed in the European CEB-FIP Model Code 1990. On the other hand, the Mises model is absolutely unable to reproduce the tensile mechanical response of the concrete. Moreover, the proposed isotropic damage model, characterized by a finite value of the crashing energy, appears more suitable than the elasto-plastic one to simulate the masonry behavior in compression. In figure 5, the plastic and the damage stress-strain relationship is plotted for compressive stresses, illustrating the material response for loading-unloading cycles.

In the following, different numerical analyses are developed using the above described material models in order to study the arch behavior considering the no-tension model for tensile stresses and the plastic or damage models for the compressive stresses. Thus, in order to perform accurate stress analyses, the elements of the arch subjected to tensile and compressive stresses are determined and modeled adopting the no-tension and the plastic or damage models, respectively.

The softening curve, adopted in the damage model, is based on crashing energy by the definition of the failure band width of the element. A crashing energy regularization technique has been used to avoid the pathological mesh sensitivity of the finite element response in presence of strain localization. Under the assumption that inelastic strains localize into a band having the width

of one element, the material crashing energy density is scaled according to the element size so that the correct failure energy is dissipated within the band. One of the features of the proposed model is that the material crashing energy density depends on a single scalar parameter and it can be easily scaled without affecting the pre-peak behavior. Following the European CEB-FIP Model Code 1990, the failure energy in compression is taken equal to $G_f^c=200$ MPa mm, while the crack band width is set about equal to three times the maximum aggregate size $h_b=50$ mm.

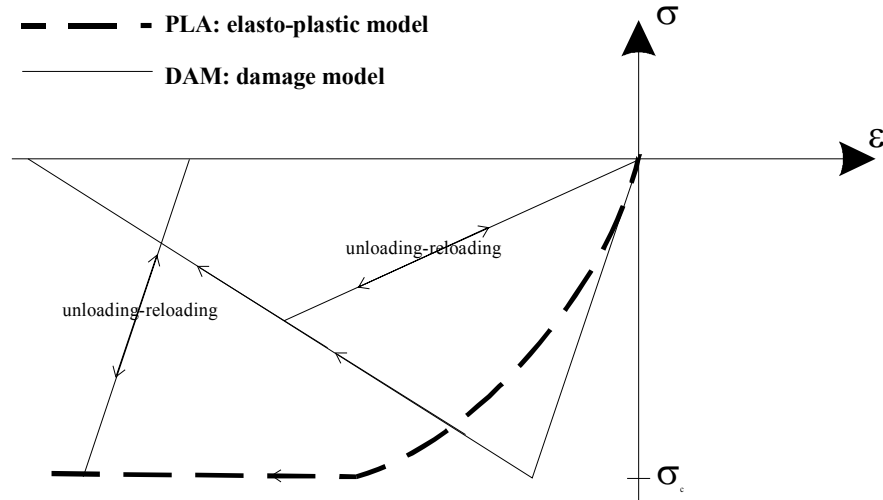


Figure 5. Stress-strain relations accounting for the plastic or the damage evolution.

Numerical Study Of The Arches

Finite element analyses are developed to study the mechanical response of the unreinforced and reinforced arches. To this end, the FEAP code is used. In particular, plane stress two-dimensional analyses are performed.

The actual geometry of the arch, constituted by six concrete blocks, is modeled using four nodes quadrilateral elements. The interfaces between two adjacent blocks are modeled by four node no-tension elements; thus, a finite width of the interfaces is considered. In figure 6 the adopted mesh, the position of the interfaces and the constraints conditions are reported.

The mechanical response of the unreinforced arch is investigated considering a linear elastic constitutive model for the concrete material since very low values of the stress are present in the blocks when the collapse mechanism occurs.

A nonlinear step by step analysis is performed using the arc-length technique [17]; in fact, the procedure is able to determine at each time increment a new point of the equilibrium path and, thus, the value of the multiplier of the vertical load prescribed at the node corresponding to the position of the hydraulic jack. In figure 7, the arch deformation is represented when the displacement of the loaded node is equal to 0.12 mm. By a comparison between the figure 2, reproducing the experimental arch deformation, and figure 7, it can be pointed out that the four hinges collapse mechanism, obtained by the numerical simulation, is in perfect accordance with the one recovered from the experimental test.

In figure 8, the mechanical response of the unreinforced arch is represented in terms of the vertical load – vertical displacement diagram. It can be emphasized that the load tends to a limit value equal to 2 kN that corresponds to the collapse load obtained experimentally. Thus, a very good accordance between the numerical and experimental results, both in terms of collapse mechanism

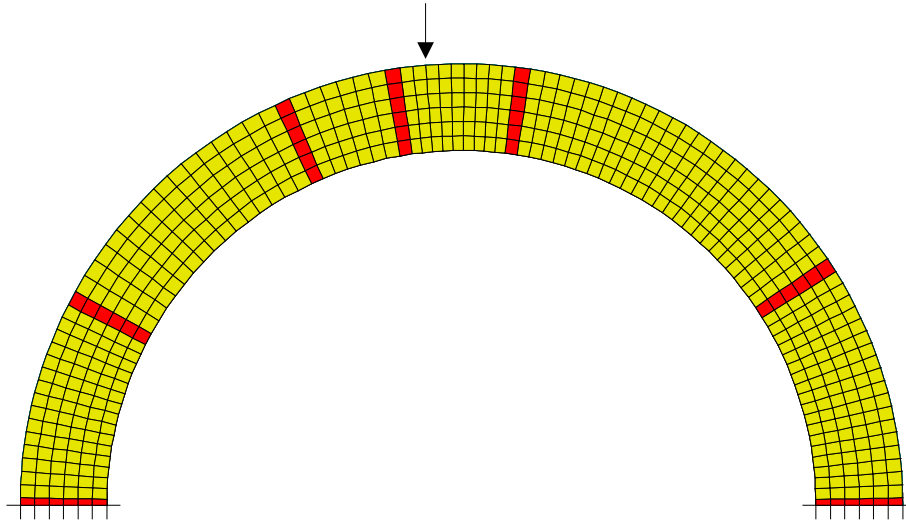


Figure 6. Arch discretization: geometry and constraints.

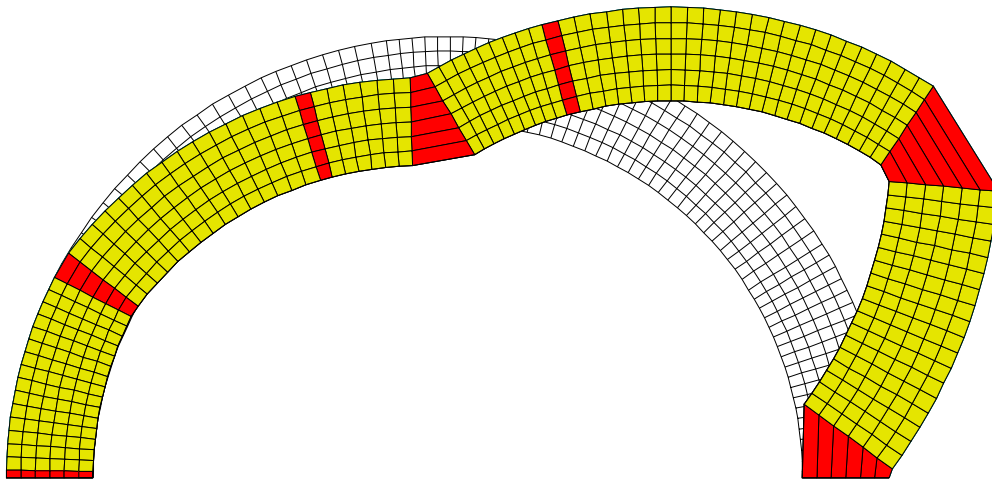


Figure 7. Deformation of the unreinforced arch at collapse.

and collapse load, can be noted.

Then, the arch reinforced by FRP sheets on the extrados is analyzed to evaluate the influence of the reinforcement on the mechanical behavior of the structure. Two nodes truss elements are adopted to model the FRP sheets. A perfect adhesion between the reinforcement and the blocks is assumed so that slipping or opening between the FRP and the concrete is not allowed. A linear elastic material is adopted for the reinforcement, the no-tension model is considered for the interfaces, while the linear and nonlinear models, introduced in the previous section, are adopted for the blocks.

Four analyses are developed adopting the following different constitutive models for the blocks:

- LIN linear elastic constitutive model;
- NTM no-tension model; it considers no tensile strength with linear elastic behavior in compression;
- PLA elasto-plastic Von Mises model for the parts in compression and no-tension model for the ones in tension,
- DAM damage model for the parts in compression and no-tension model for the ones in tension.

The nonlinear evolutive elasto-damage model is solved within the FEAP code adopting an implicit back-ward Euler time integration. In particular, the tangent stiffness method developed in [18, 19] is adopted to solve the no-tension nonlinear equilibrium problem. A step by step analysis is performed adopting the arch-length technique, able to automatically increase or decrease the multiplier value of the external force prescribed at the node characterized by an eccentricity of 80 mm with respect to the keystone.

The deformed configurations of the reinforced arch, obtained considering the different

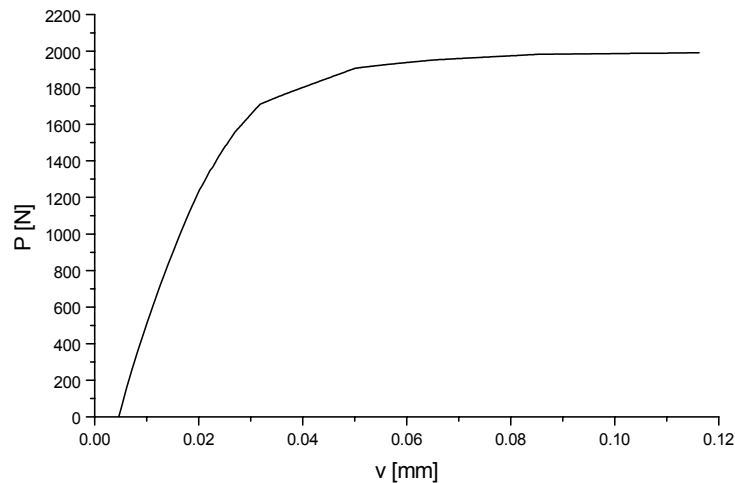


Figure 8. Mechanical response of the unreinforced arch.

models for the blocks, are very similar each other. In figure 9, the deformation of the reinforced

arch, occurring for the vertical displacement equal to 10 mm, is reported for the DAM model. It can be emphasized that only three hinges are possible, in fact, because of the presence of the stiff FRP reinforcement, the formation of the four hinges is not possible and, thus, the definition of a collapse mechanism is forbidden. Moreover, the position of the three hinges obtained for the reinforced arch is changed with respect to the position of the four hinges determined for the unreinforced arch; in fact, the three interface openings occur between the blocks under the external load (i.e. between blocks 3 and 4) and at the bases of the arch (i.e. between support and block 1 and between support and block 6). In figure 9, the equilibrium scheme of the applied force and reactions is also reported.

In figure 10, the mechanical responses, obtained adopting the different material models introduced above, are plotted in terms of vertical displacement of the loaded node versus the applied force. It can be emphasized that the no-tension model leads to an overall linear behavior of the structure; in fact, during the loading process the fractured parts of the arch does not change, i.e. there is no variation of the cracked zone; while the zones in compression behave as a linear elastic material. The elasto-plastic and the damage models present nonlinear responses. In particular, as it can be expected, a softening behavior is recovered considering the damage effect. The peak load is about 700 kN, which is more than twice the experimental collapse load. In fact, the real structure presents some construction defects that play a crucial role for the collapse behavior, as it clearly occurred during the second experimental test. Thus, the numerical results obtained considering the damage effect can be considered satisfactory.

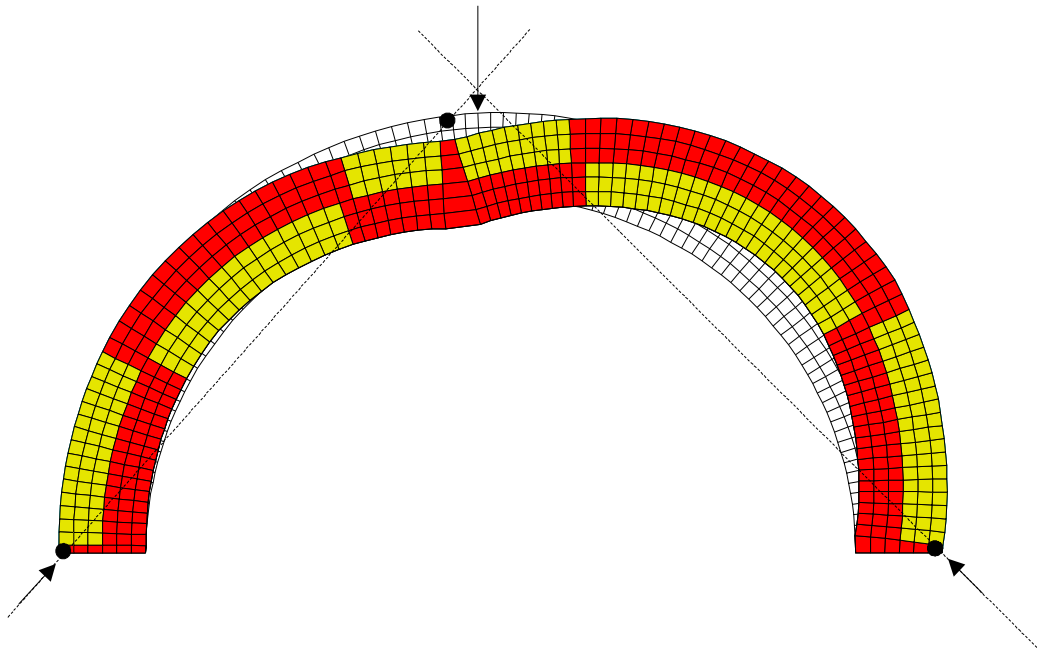


Figure 9. Deformed configuration of the reinforced arch.

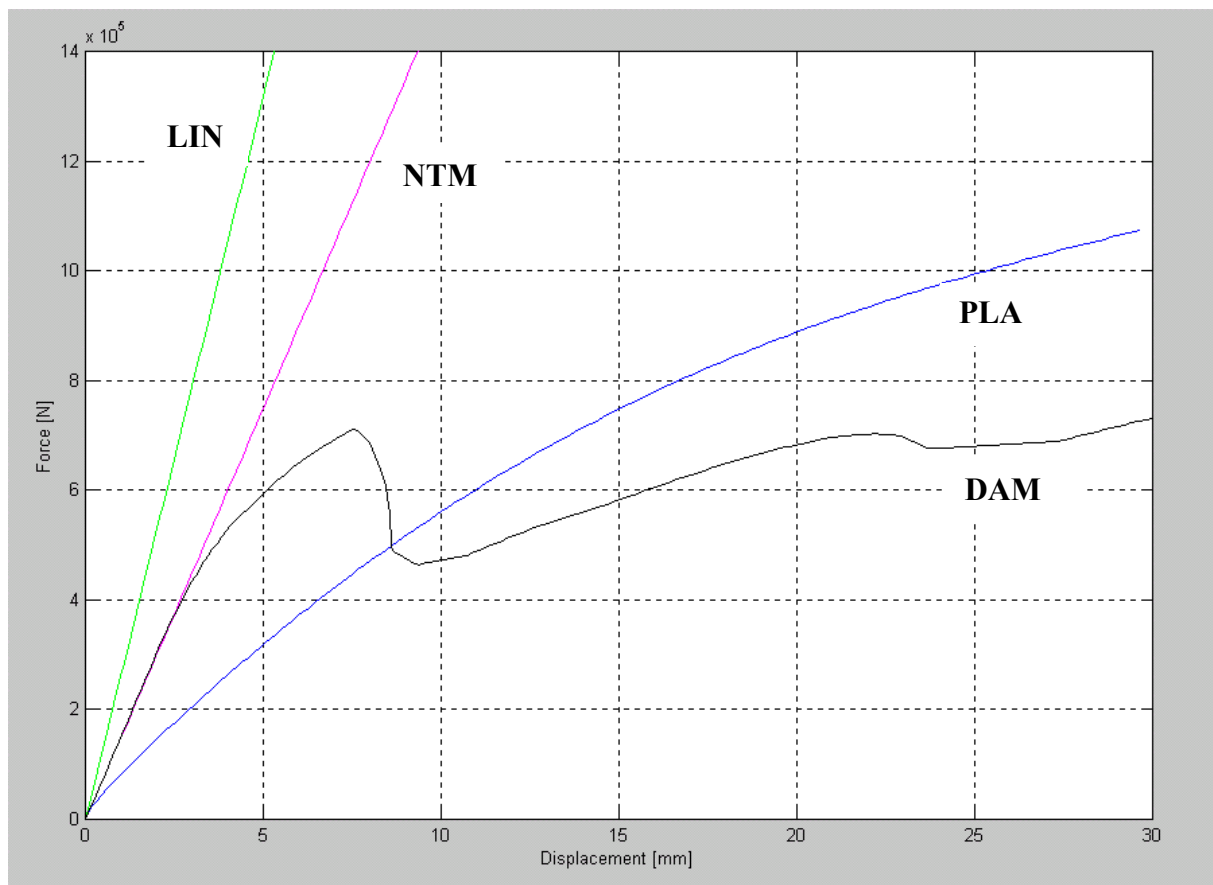


Figure 10. Mechanical response of the reinforced arch.

Conclusions

The presented study points out the effectiveness of carbon FRP composites in strengthening masonry arches realized by blocks without mortar. In the analyzed cases, the increase of bearing capacity of the arch is about 10000%. Furthermore, the numerical simulations are able to predict the behavior of unreinforced and reinforced arches; in fact, in the first case the collapse mechanism and the collapse load obtained numerically is in perfect agreement with the experimental evidences. Moreover, for the reinforced arches, the computations are able to predict the overall behavior even if an over-estimation of the collapse load is obtained.

Acknowledgments: The authors are grateful to the GEOLAB Laboratory for the technical support during the experimental tests. The financial support of the Ministry of University and Research (MURST) are gratefully acknowledged.

References

1. Croci, G., Ayala, D., Asdia, P. and Palombini, F. (1987), "Analysis on shear walls reinforced with fibres", *IABSE Symp. on Safety and Quality Assurance of Civil Engineering Structures*, Tokyo, Japan.
2. Schwegler, G. (1994), "Masonry construction strengthened with fiber composites in seismically endangered zones", *Proceedings of 10th European Conference on Earthquake Engineering*, Vienna, Austria.
3. Saadatmanesh, H. (1994), "Fiber composites for new and existing structures", *ACI Structural Journal*, **91**, 346-354.
4. Ehsani, M. R. (1995), "Strengthening of earthquake-damaged masonry structures with composite materials", In *Non-metallic (FRP) Reinforcement for Concrete Structures*. Ed. L. Taerwe, 680-687.
5. Laursen, P. T., Seible, F., Hegemier, G. A. and Innamorato, D. (1995), "Seismic retrofit and repair of masonry walls with carbon overlays", In *Non-metallic (FRP) Reinforcement for Concrete Structures*. Ed. L. Taerwe, 616-623.
6. Seible, F. (1995), "Repair and seismic retest of a full-scale reinforced masonry building", *Proceedings of the 6th International Conference on Structural Faults and Repair*, Vol. 3, 229-236.
7. Triantafillou, T. C. (1996), "Innovative strengthening of masonry monuments with composites", *Proceedings of 2nd International Conference Advanced Composite Materials in Bridges and Structures*, Montreal, Quebec, Canada.
8. Triantafillou, T. C. and Fardis, M. N. (1997), "Strengthening of historic masonry structures with composite materials", *Materials and Structures*, 1997, **30**, 486-496.
9. Luciano, R. and Sacco, E. (1997), "Homogenization technique and damage model for old masonry material", *International Journal of Solids and Structures* **34**, 3191-3208.
10. Luciano, R. and Sacco, E. (1998), "Damage of masonry panels reinforced by FRP sheets", *International Journal of Solids and Structures* **35**, 1723-1741.
11. Marfia, S. and Sacco, E. (2001), "Modeling of reinforced masonry elements", *International Journal of Solids and Structures* **38**, 4177-4198.
12. Croci, G. and Viskovic, A. (2000), "L'uso degli FRP di fibra aramidica per il rinforzo della Basilica di San Francesco di Assisi", *Proc. of Mechanics of masonry structures strengthened with FRP – materials*, Venezia, Italy.
13. Como, M., Ianniruberto, U. and Imbimbo, M. (2000), "La resistenza degli archi murari rinforzati con fogli in FRP", *Proc. of Mechanics of masonry structures strengthened with FRP – materials*, Venezia, Italy.
14. Zienkiewicz, O. C. and Taylor, R. L. (1991), *The Finite Element Method, 4th edition*, Mc Graw-Hill, London.
15. Luciano, R., Marfia, S., Rinaldi, Z. and Sacco, E. (2001), "Application of advanced composites for the reinforcement of masonry arches", *Proceedings of CICE 2001 International Conference on FRP Composites in Civil Engineering*, Hong Kong, China.
16. Sacco, E. (1990), "Modellazione e calcolo di strutture in materiale non reagente a trazione", *Atti della Accademia dei Lincei, Serie IX*, I (3).

17. Crisfield, M. A. (1991), *Non-linear Finite Element Analysis of Solids and Structures. Vol. I*. John Wiley & Sons LTD, England.
18. Lucchesi, M., Padovani, C. and Pagni, A. (1994), “A numerical method for solving equilibrium problems of masonry-like solids”, *Meccanica* **29**, 175-193.
19. Alfano, G., Rosati, L. and Valoroso, N. (2000), “A numerical strategy for finite element analysis of no-tension materials”, *Int. J. Numer. Methods Engng.* **48**, 317-350.